

The Kinetics of Penetration of Grafted Polymers into a Network

M. Geoghegan,^{†,‡,§} C. J. Clarke,^{*,||} F. Boué,[†] A. Menelle,[†] T. Russ,[‡] and D. G. Bucknall[⊥]

Laboratoire Léon Brillouin CEA-CNRS, CE-Saclay, F-91191 Gif-sur-Yvette Cedex, France, Fakultät für Physik, Universität Freiburg, Hermann-Herder-Strasse 3, D-79104 Freiburg, Germany, Polymers and Colloids Group, Cavendish Laboratory, Madingley Road, University of Cambridge, Cambridge CB3 0HE, U.K., and Rutherford Appleton Laboratory, Chilton, Didcot, Oxfordshire OX11 0QX, U.K.

Received December 29, 1998; Revised Manuscript Received May 6, 1999

ABSTRACT: We present the results of a neutron reflectometry study of the kinetics of penetration of a grafted polymer layer into a permanently cross-linked, chemically identical network. The polymer used was polystyrene. Initially the grafted chains are completely excluded from the network, and the interface between them is sharp. The segment density profile was measured after a series of annealing times to follow the kinetics of penetration. The range of annealing times was extended over 9 orders of magnitude by using time–temperature superposition. We observe a slow approach to equilibrium, in good agreement with theory, which predicts this to be logarithmic in time. The kinetics of penetration is slower for more densely cross-linked networks and for greater brush grafting densities. We also note a grafting density dependence of the equilibrium profile but, somewhat unexpectedly, no dependence on the density of cross-links.

Introduction

The properties of many composite materials are dominated by the nature of the interfaces between the different phases, since interfaces are most susceptible to deformation or fracture. In plastic or rubber composites, one means of modifying the properties is to anchor polymers at the interface.^{1,2} At a polymer–polymer interface, diblock copolymers are typically used so that one block lies in each of the bulk phases. At a polymer–inorganic interface a polymer chain which is physically or chemically attached to the inorganic material and whose free end is entangled in the bulk polymer provides the reinforcement. There have been several studies investigating the fracture toughness^{3–6} and other properties, such as sliding friction^{7–12} of interfaces reinforced in this manner. The extent and rate of penetration of the grafted chains into the bulk polymer crucially govern the strength of the interface and the healing of reinforced interfaces after fracture.^{12–14} Thus any commercial means of strengthening materials by reinforcing the interface with anchored polymers must address the issue of how to achieve maximum interpenetration.

A technologically important example is the interface between a cross-linked network (a rubber) and a solid substrate coated with grafted polymers. A substantial amount of experimental work has been performed to measure macroscopic quantities of importance such as the fracture toughness, or the shear stress–slip velocity relationship.^{3–5,7–11} Theoretical work provides models in terms of molecular conformations.^{6,12,13,15–17} However despite several authors^{4,5,15} calling for experiments

which can probe the structure of grafted layers on the molecular level to link these together, there has been little work to date. In this paper, we attempt to bridge this gap. We report an experimental study of the kinetics of penetration of grafted polymers into a network using neutron reflectometry in order to determine information on the molecular conformations at the interface. This extends earlier work in which the matrix was a high molecular weight (M_w) homopolymer.¹⁸ We begin by summarizing the current position of theory and experiment.

Current Experiments and Models. As a first experimental attempt to understand the kinetics of brush penetration into a rubber system, Clarke¹⁸ used neutron reflectometry to study the penetration of a polystyrene brush into a high M_w (8×10^6) homopolymer. In these experiments a two-stage process was observed in which the brush rapidly penetrated the matrix before slowing down in its approach to equilibrium. The homopolymer can be likened to a network in many respects because its terminal time¹⁹ is much greater than the experimental time scale. Nevertheless, one cannot assume that a high M_w homopolymer is a satisfactory approximation to a network. A major difference concerns heterogeneity. The distribution of entanglements in high polymers is given by the entanglement length, which is constant throughout the material. This distribution exists also in networks. However, on top of this, one must also include the distribution of fixed entanglements (cross-links) which is usually polydisperse and always anisotropic (except, perhaps, in the case of some esoteric rigid networks or temporary physical gels).

Geoghegan et al.²⁰ have used neutron reflectometry to look at the penetration of linear homopolymers into networks. For long linear polymers, providing the network was not too cross-linked, they found that the interfacial profile consists of two components, a sharp interface (which was unexpected) and a certain amount of penetration. The penetration was not surprising and

* Corresponding author. Present address: Unilever Research, Colworth House, Sharnbrook, Bedfordshire MK44 1LQ, U.K.

[†] Laboratoire Léon Brillouin CEA-CNRS.

[‡] Universität Freiburg.

[§] Present address: Physikalische Chemie II, Universität Bayreuth, D-95440 Bayreuth, Germany.

^{||} University of Cambridge.

[⊥] Rutherford Appleton Laboratory.

was of the length scale expected by simple mean field theory.

The (equilibrium) extent of interdigitation of a brush into a chemically identical network has been considered analytically, by Brochard-Wyart et al.⁶ using a simplified Flory type argument, and an analogy between a rubber and a melt of short chains. Their work was improved on by Ligoure,¹⁴ who used a self-consistent field approach with a parabolic brush profile to allow a quantitative description of the statistics of chain segments embedded in the network. Different regimes were found, depending on the grafting density (i.e. the number of chains per unit area, σ) and the ratio of the number of monomers per cross-link (P) to the number of monomers in the grafted chains (N). As the grafting density is increased, there is an energy penalty associated with the swelling of the network by the grafted chains. Thus at a point where this energy penalty balances the entropy cost of excluding grafted chain segments from the brush, there is a crossover from total to partial interdigitation. In the latter situation the brush is divided into two regions: close to the substrate, the brush chains form a passive dry layer (there is no mixing with the matrix) in the melt state; above a certain distance, the chains penetrate the elastomer and form a swollen layer. The free end of the chain may be located in either layer. The crossover occurs at a grafting density given by

$$\sigma = \frac{4\sqrt{2}}{3\pi b^2 \sqrt{P}} \quad (1)$$

where b is the Kuhn segment length. The kinetics of penetration of anchored polymer chains into a cross-linked network has been investigated theoretically by O'Connor and McLeish^{15,16} (hereafter referred to as O & M), and by computer simulation.¹⁷ O & M^{15,16} considered grafted chains, initially completely excluded from a permanently cross-linked network. They discuss two regimes, low and high grafting density. In the low grafting density case

$$\sigma \ll \sigma^* = \frac{1}{b^2 N} \quad (2)$$

In this regime the grafted chains initially lie in an unentangled layer at the substrate with their free ends some distance away from the grafting point. When annealing is commenced, the free end gains entropy by penetrating the network. However, most of these will enter the network some distance from the grafting point, so that a length of chain remains on the substrate. O & M have described this metastable state, shown schematically in Figure 1, as a "strawberry runner" by analogy with plants having trailing surface roots. The penetration of the free ends into the unentangled surface layer of the network is governed by Rouse dynamics¹⁹ and has a characteristic time given by

$$\tau_d \approx \tau_1 \left(\frac{d}{2b} \right)^4 \quad (3)$$

where k_B is Boltzmann's constant and T is the absolute temperature. The tube diameter for the brush chains (d) is smaller than the bulk value of ~ 80 Å, due to the extra confinement from the substrate, and is given by the thickness of the brush layer (see Figure 1). τ_1 is the relaxation time of a segment¹⁹ (the Kuhn relaxation

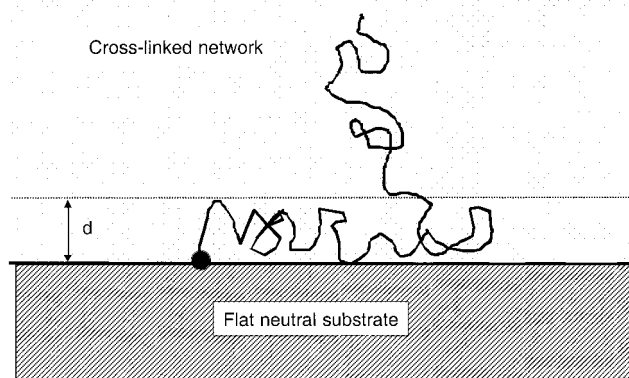


Figure 1. Schematic diagram showing a polymer in the "strawberry runner" configuration.

time). Above the glass transition temperature, this is very short, (on the order of 10^{-3} s in our experiments²¹). Once embedded in the surface layer, the chain end will bury itself in the network in a time

$$\tau_{N_t} \approx \tau_1 N_t^2 \quad (4)$$

where N_t is the number of monomers that penetrate the network.

The equilibrium conformation of a grafted chain is one in which there is no "runner" on the substrate; i.e., the free end penetrates the network directly above its grafting point. To reach this, the free end has to retract along its original tube in the network and re-enter near its grafting point. This is similar to the breathing mode relaxation of star polymers.^{22,23} The time scale for this process is given by the characteristic occupation time of a particular tube. O & M estimate that this relaxation time is

$$\tau_R \sim \tau_{N_t} \exp\left(\frac{\alpha^2 b^2 N}{6a^2}\right) \quad (5)$$

where α is a numerical constant of order unity and a is the characteristic distance between cross-links in the network.

In the high grafting density regime, grafted chains overlap and are stretched. There will be a layer of pure melt brush between the substrate and the network, whose thickness is reduced as the brush chains penetrate. The dynamics are still slow for two reasons: (i) just as for dilute grafted chains, entanglements will require reconfigurations to proceed via star-arm retraction dynamics; (ii) there will also be entanglements in the melt brush layer below the network, which are maintained as the free end penetrates into the network; the topological structure in the melt layer is compressed, which produces a higher entanglement density and controls the slow cooperative dynamics of the brush. The exponentially slow starlike diffusion again sets a time scale.

Deutsch and Yoon¹⁷ have performed Monte Carlo simulations to study the kinetics of penetration of a grafted polymer layer into a network. They considered a very highly cross-linked network (where the distance between entanglements is equal to the Kuhn segment length) and studied chains grafted at both ends as well as just one. They considered only one grafting density but varied the length of the grafted chain and the

interaction parameter between the grafted chain and the wall. They also found a two-stage process. Since, in their simulations, the configuration of the grafted chain is known at each point in time, they were able to observe the strawberry runners directly and also determine the distance between the grafting point and the point of entry into the network as a function of time.

For the case corresponding to our experiments (i.e. no interaction between the grafted chain and the wall, and without a strongly entangled brush layer), they found a rapid initial penetration followed by a slow relaxation to equilibrium. Their simulations showed that the number of monomers that penetrate the network initially follows a $t^{1/2}$ growth. After a time $\sim \tau_1 N^2$, (the time scale predicted by O & M for a chain to bury itself in the network, leaving only a stretched runner on the surface, eq 4) there is a crossover and the number of segments of the grafted chains inside the network increases as $\ln(t)$. Most of the interfacial toughness is gained in the first stage. Similarly, Reichert and Brown³ found experimentally an almost instantaneous increase in fracture toughness followed by a slow increase over a period of days.

Ligoure¹⁴ considers a different effect of the kinetics of interdigitation (neglecting the topological constraints of O & M's model). He finds an energy barrier for interdigitation that the system has to overcome in order to reach the equilibrium conformation. However this effect is not important for $N < 75P$. In our case $N = 900$, and the smallest value of P is 45, so we did not consider it further.

Deruelle et al. have studied adhesion at the interface between a solid surface coated with a layer of grafted chains and an elastomer, by measuring the strain energy release rate (G) with the JKR method.^{4,5} Their principal result is that G passes through a maximum as the grafting density increases, which they could explain in terms of the penetration of the grafted chains into the network. For a fixed grafting density, greater spacing between cross-links produces enhanced adhesion, which they propose is due to greater interpenetration. However they are not able to verify this since their experiments measured only macroscopic quantities and are not able to observe the microscopic chain conformations.

Deruelle et al. also found that the contact time between the brush and the network before unloading was commenced had an effect on their results; there was a significant change in the interface on a time scale of 30 min (~ 150 K above T_g for their system), but little change beyond that. However they were not able to study longer times accurately. They interpreted their results in terms of "active connectors", i.e., portions of the grafted chains that penetrate the network. Their data suggests that the active connector length is independent of the length of the grafted chain; i.e., only a portion of the chain forms an active connector. This suggests that they have not reached true equilibrium but only the metastable state with partial interdigitation. Although they found no evidence for slow rearrangement kinetics as proposed by O & M, they could not exclude the possibility.

Experimental Section

Grafted Layer Preparation. Permanently grafted polymer layers were prepared on oxide coated silicon wafers using a well-established procedure.²⁴ Briefly, monodispersed carboxy terminated deuterated polystyrene (molecular weight 100 000)

Table 1. Summary of Sample Sets

set	grafting density, σ (\AA^{-2})	$a/\sigma^* = \sigma b^2 N$	monomers per cross-link
1	3.4×10^{-4}	14	45
2	2.0×10^{-4}	8	92
3	3.4×10^{-4}	14	92
4	3.4×10^{-4}	14	197
5	2.0×10^{-4}	8	325
6	3.4×10^{-4}	14	461

was obtained from Polymer Laboratories. The end group was then converted to a triethoxysilane group, which bonds strongly to silicon oxide. Single-crystal silicon wafers (5 cm diameter) were cleaned with toluene and methanol. The native oxide layer was stripped with hydrofluoric acid. The wafers were then etched in oxygen plasma for 3 min, to regrow a uniform oxide layer. This was characterized by ellipsometry and found to be 30 ± 5 Å thick. The functionalized polymer was spin coated from toluene solution to form a layer ~ 300 Å thick. The wafers were then annealed overnight in a vacuum oven to allow the end groups to graft to the substrate. The ungrafted polymer was removed by washing several times with toluene. The thickness of the layer was measured by ellipsometry, from which the grafting density could be deduced. The grafting density was varied by changing the annealing temperature: annealing at 125 °C produced a 30 ± 5 Å thick brush (2.0×10^{-4} chains \AA^{-2}) and at 197 °C, 50 ± 5 Å (3.4×10^{-4} chains \AA^{-2}).

Network Preparation. The synthesis of the polystyrene networks has been described in detail.^{20,25,26} Briefly, it is a three-stage process using a Friedel–Crafts reaction and then an exchange reaction to functionalize the polystyrene with an aminomethyl (NH_2CH_2) group on the aromatic ring at random points along the chain. In the final stage, the polystyrene is cross-linked by adding terephthalaldehyde. This method permits a wide range of cross-linking densities, from heavily cross-linked (30 monomers per cross-link) to lightly cross-linked films (up to 500 monomers per cross-link). Nonfunctionalized polystyrene will not cross-link in the presence of the aldehyde so that there is no possibility of the grafted chains linking to the network during annealing. It has the further advantages that networks can be created with negligible sol fraction present and that cross-linking can proceed during the spin casting onto the glass substrate. These networks will necessarily be heterogeneous; i.e., there will be regions of greater and lesser cross-linking. This is also the case for end-linked networks such as the PDMS elastomer studied by Deruelle et al.⁵ but the distribution of cross links will be wider in our case.

Samples were prepared by floating the network from the glass substrate and onto the surface of distilled or de-ionized water. They were then picked up onto the brush-covered silicon substrates and left to dry. The samples were annealed in a vacuum oven at various temperatures above the glass transition temperature of polystyrene (100 °C) for a range of times.

The grafting and cross-linking densities used in our experiments are summarized in Table 1. For our grafted chains $N = 900$ and $b = 6.7$ Å giving a value of 2.5×10^{-5} \AA^{-2} for $1/b^2 N$, (eq 2). Thus our grafted layers are in the high grafting density regime described by O & M. They also fall into the regime of total interdigitation at equilibrium according to Ligoure.¹⁴

Neutron Reflectometry. Neutron reflectometry (NR) is now a well-established and commonly used tool in the study of polymers at surfaces and interfaces. It measures the neutron scattering length density as a function of distance from a surface with resolution of ~ 5 Å. It is particularly suitable for polymers since high contrast can be obtained by labeling one component with deuterium. The technique has been described in detail elsewhere.²⁷ The reflectivity data were collected at the CRISP time-of-flight reflectometer at the ISIS facility, Rutherford Appleton Laboratory, and at the EROS time-of-flight reflectometer, situated at the Laboratoire Léon Brillouin. The data were analyzed by producing fits from model profiles, which were refined to minimize χ^2 by a simplex fitting

Table 2. WLF Time–Temperature Scaling at a Reference Temperature of 150 °C

temperature (°C)	time (min)	scaled time (s)
119	20	0.27
122	15	0.64
127	20	4.7
128	60	19
135	90	2.1×10^2
148	15	6.0×10^2
143.5	120	2.0×10^3
154	120	1.5×10^4
149.5	300	1.6×10^4
150	300	1.8×10^4
162.5	180	8.3×10^4
179.5	9900	3.8×10^7
180	9660	3.9×10^7

routine.²⁸ The model profiles were usually either an error function or a hyperbolic tangent at the substrate (there is no noticeable difference between the two). Maximum entropy methods^{29,30} (MaxEnt) were also used as a check. Although there are uncertainties in interpreting reflectivity data because of the loss of phase information, the prior knowledge of the scattering length densities and the fact that the grafted chains remain attached to the substrate are sufficient to remove the ambiguities, so that we can be confident of the validity of our fits and profiles.

Results

Six sets of experiments were carried out, using four cross-link densities and two grafting densities. Each set consisted of reflectometry experiments (and hence brush profiles) for a range of annealing times, from unannealed to several days at high temperature. To maximize the range of different times that could be studied, time–temperature superposition was used. Different temperatures were placed on a single time scale, by using the WLF equation³¹ with a reference temperature of 150 °C. We used the following equation for the rescaled time:

$$t_s = \frac{tT}{W} \exp\left(\frac{-0.8}{0.22 + 4.8 \times 10^{-4}(T - T_g)}\right) \quad (6)$$

where t is the actual annealing time and T_g is the glass transition (absolute) temperature of the polystyrene. The constants 0.22 and $4.8 \times 10^{-4} \text{ K}^{-1}$ are universal, and the constant 0.8 is specific to polystyrene.³¹ W is a constant and ensures that $t_s = t$ at 150 °C. The factor T , outside the exponential, does not come from the WLF equation but is included to take into account the temperature dependence of the monomer mobility. The actual temperatures and scaled temperatures are compared in Table 2. The range of times covers 9 orders of magnitude. Most sets had measurements at five different times, apart from set 3 which consists of nine different times, to follow the kinetics in detail. From here on, the scaled time rather than the actual time is used.

Figure 2 shows the reflectivity data and best fits for set 1. The other data sets have similar reflectivity curves, and similar quality fits. All but three fits had values of $\chi^2 < 10$, with most between 1 and 3. Fits for the unannealed samples were in general the poorest. Figures 3–8 show the profiles for all the data sets derived from the fits. We discuss these as follows: We first make some general observations, pertinent to all the data sets. Second, we discuss in detail set 3, which has the most measurements and hence the best time resolution. Next, we consider the effect of cross-linking

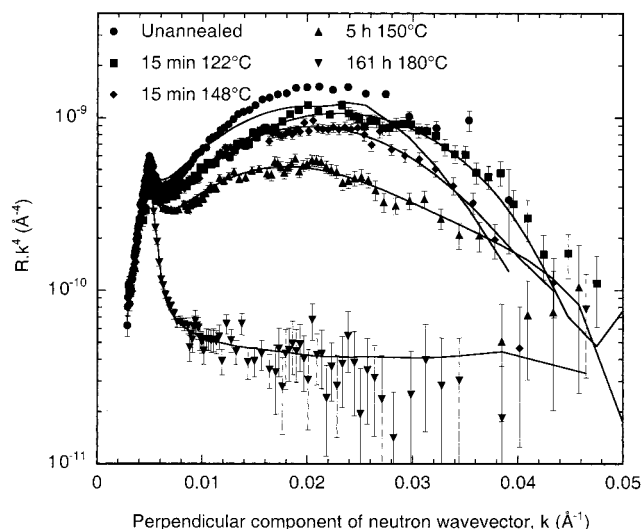


Figure 2. Reflectivity data (points) and best fits (lines) for data set 1 ($\sigma = 3.4 \times 10^{-4} \text{ Å}^{-2}$, $P = 45$) for a range of annealing times. These times are the actual (as opposed to scaled) annealing times.

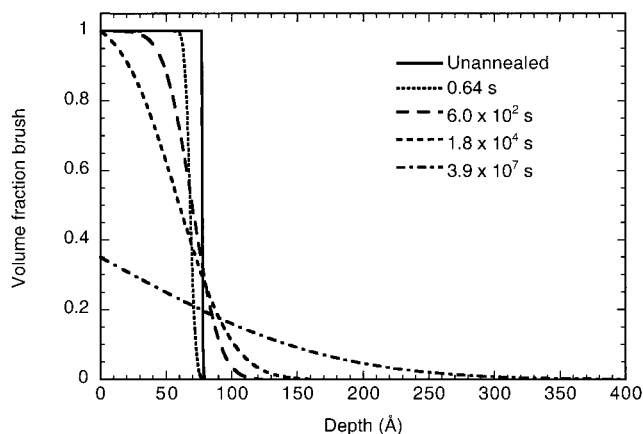


Figure 3. Profiles for set 1 ($\sigma = 3.4 \times 10^{-4} \text{ Å}^{-2}$, $P = 45$) derived from the fits shown in Figure 2 for various scaled annealing times.

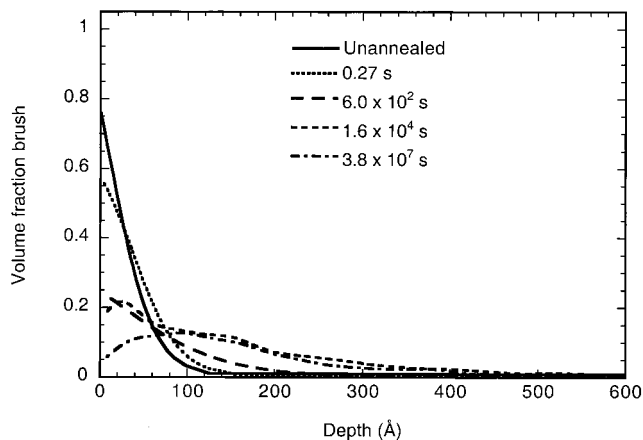


Figure 4. Profiles for set 2 ($\sigma = 2.0 \times 10^{-4} \text{ Å}^{-2}$, $P = 92$) derived from fits to the reflectivity data. The two longest anneals were fitted using MaxEnt.

density by comparing sets 1, 3, 4, and 6. Fourth, we examine the effect of grafting density with reference to sets 2 and 3. In addition, we compare the profiles in the network with those in a homopolymer matrix.

General Comments. In each case, the interface between the grafted layer and the network is initially

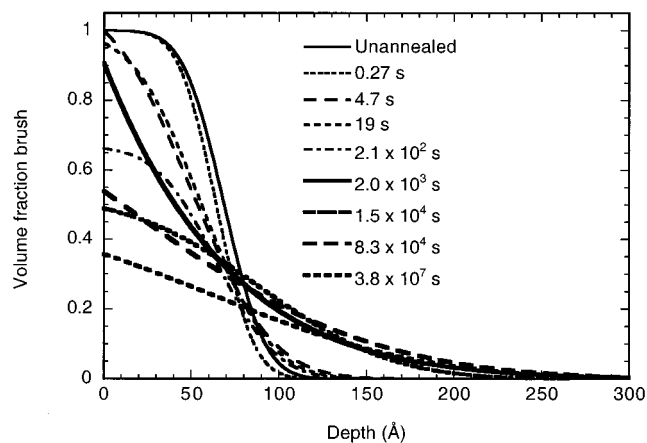


Figure 5. Profiles for set 3 ($\sigma = 3.4 \times 10^{-4} \text{ Å}^{-2}$, $P = 92$) derived from fits to the reflectivity data.

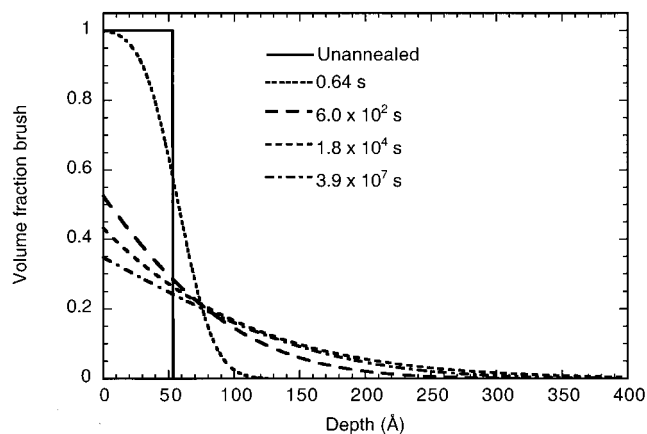


Figure 6. Profiles for set 4 ($\sigma = 3.4 \times 10^{-4} \text{ Å}^{-2}$, $P = 197$) derived from fits to the reflectivity data.

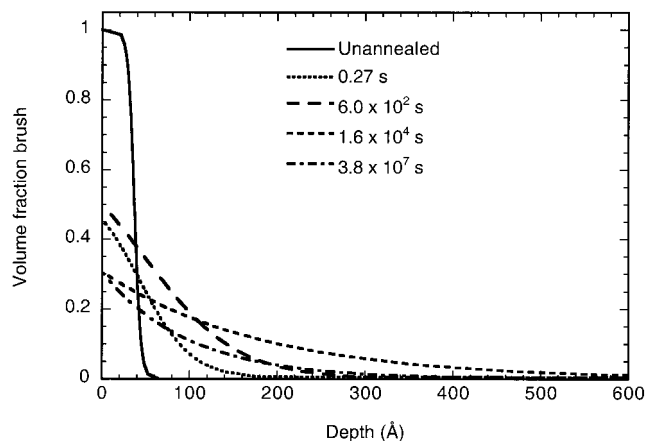


Figure 7. Profiles for set 5 ($\sigma = 2.0 \times 10^{-4} \text{ Å}^{-2}$, $P = 325$) derived from fits to the reflectivity data.

sharp, although it is slightly broadened from the ideal step function in most cases. This is due to roughness at the interface produced during sample preparation that is typically greater for networks with fewer monomers between cross-links.²⁰ In one case (set 2, Figure 4), the unannealed sample has a substrate volume fraction of 0.75 instead of 1, due to incomplete coverage of the silicon wafer by the brush, though the interface is still sharp. In every case, there is a noticeable broadening of the interface after the shortest annealing time (except for set 3 which has a broader initial interface and hence only a small change). This presumably corresponds to

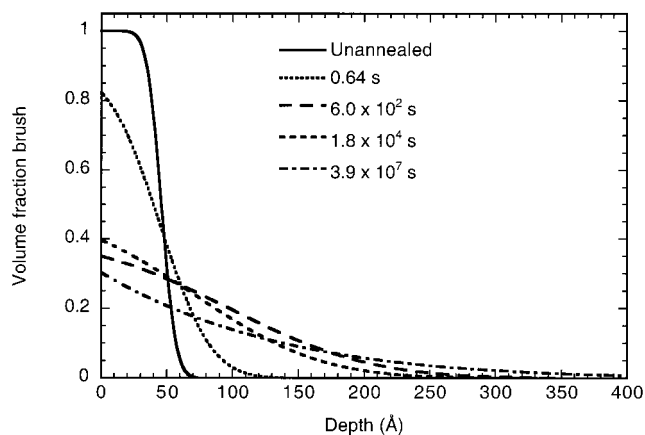


Figure 8. Profiles for set 6 ($\sigma = 3.4 \times 10^{-4} \text{ Å}^{-2}$, $P = 461$) derived from fits to the reflectivity data.

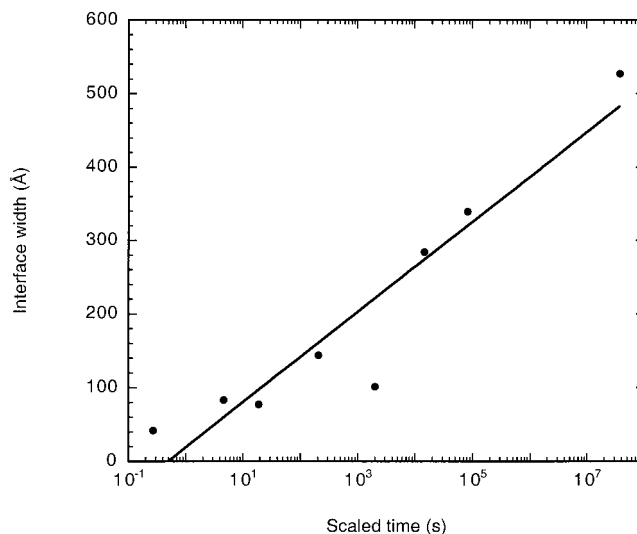


Figure 9. Plot showing the width of the interface between the brush and the network against annealing time for set 3 ($\sigma = 3.4 \times 10^{-4} \text{ Å}^{-2}$, $P = 92$). The straight line is a logarithmic fit (width $\propto \log t$).

the rapid initial penetration of the free ends into the network. The volume fraction of the grafted chains at the substrate stays at one, as expected from the “runners” model.

As annealing proceeds, we see a slow broadening of the interface and a corresponding drop in the volume fraction at the substrate in every case. Changes continue to occur even after several hours at high temperature, much longer than it takes to reach equilibrium with a homopolymer matrix.²⁴ After 3.9×10^7 s, grafted chains extend 200–250 Å ($\sim 3R_g$) into the network. We note that the profiles for the three longest annealing times for $P = 461$ (Figure 8) are similar and, likewise, the longest two for $P = 197$ (Figure 6). This suggests that equilibrium is being approached in these samples. We cannot say for certain whether we have reached equilibrium in the case of the two more cross-linked networks ($P = 92$ and 45). Unfortunately, longer annealing times are not possible due to the risk of sample degradation, so it is not possible to demonstrate unequivocally that equilibrium has been reached. We do note, however, that in set 3 ($P = 92$, Figure 5) that after 2000 s, the maximum distance of penetration of the brush into the network does not significantly change even though the actual profile does. We therefore

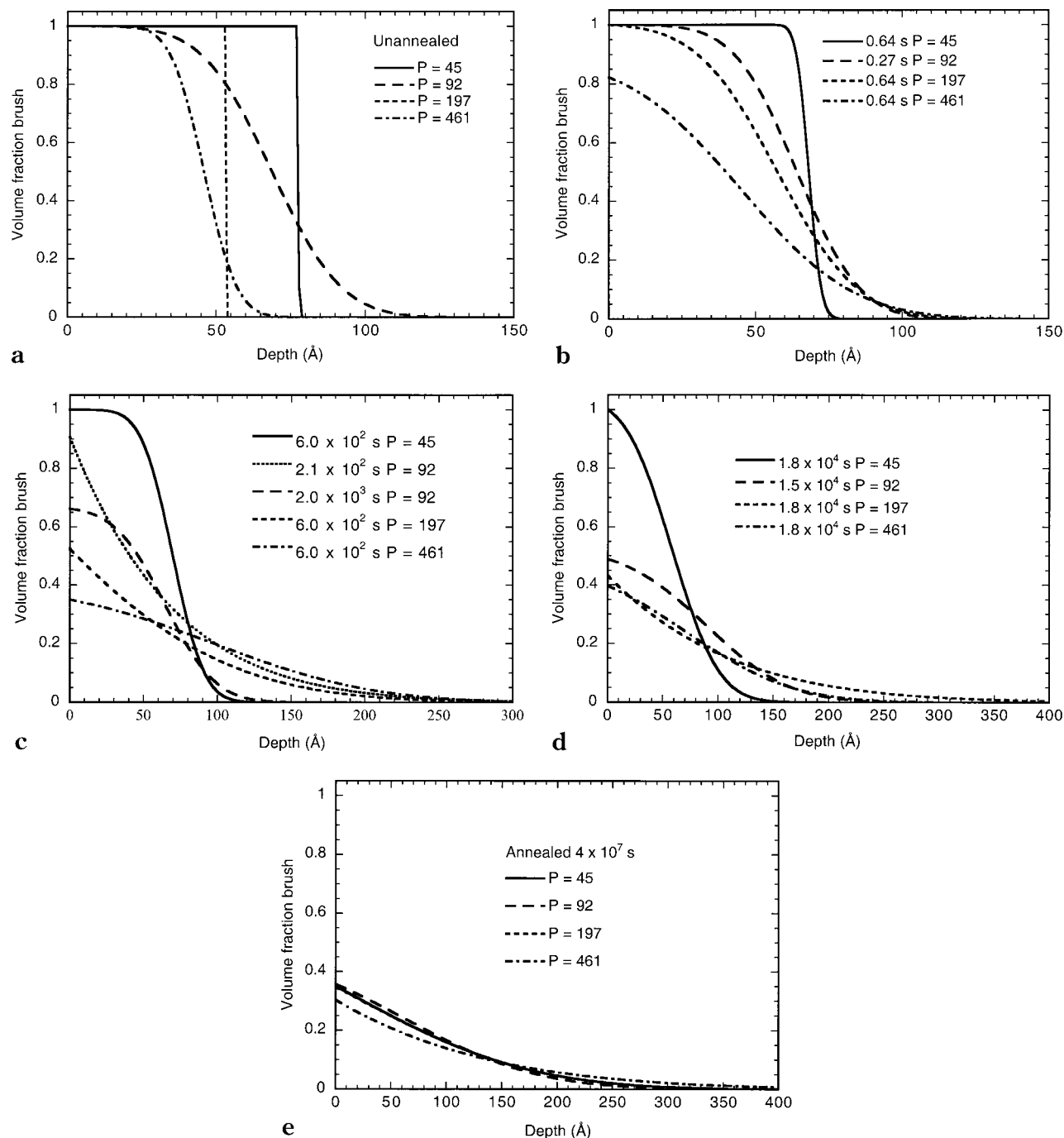


Figure 10. Brush profiles for the higher grafting density with varying cross-link densities after annealing: (a) unannealed; (b) ~ 0.5 s; (c) 6.0×10^2 s (except for $P = 92$ for which the closest annealing times were 2.1×10^2 and 2.0×10^3 s, which are both shown); (d) 1.8×10^4 s (1.5×10^4 s for $P = 92$); (e) equilibrium.

suppose that this system is close to equilibrium. We can make no such assumption for the $P = 45$ network.

Set 3. The characteristic time for the initial free end penetration is given by eq 4 and is on the order of $N_t^2 \times 10^{-3}$ s at our reference temperature. Thus for our shortest annealing time (0.27 s), chain segments with ~ 20 monomers will have already penetrated the matrix. Therefore, we cannot probe the rapid initial penetration. In any case, the resolution of the experiments (~ 5 Å) and the initial roughness of the interface makes this stage difficult to observe experimentally. A random walk of 20 steps gives an interfacial broadening of $\sim b\sqrt{20} \approx 30$ Å, which is roughly the width of the 0.27 s profile.

The profile continues to broaden steadily during annealing. The characteristic time for the breathing

mode relaxation is given by eq 5, and is on the order of 10^5 s for $N_t = 900$. This is consistent with our results, in which changes continue to occur until $\sim 10^6$ s. Figure 9 shows a plot of the width of the interface between the brush and the network (which is a measure of the interpenetration) against the logarithm of the scaled annealing time. The width is calculated from the gradient of the segment density profile when the volume fraction drops to half of its value at the substrate. The plot shows that the width increases slowly with time. Good agreement is obtained with $\text{width} \propto \log t$ (the straight line). Deutsch and Yoon¹⁷ found that the number of segments penetrating the matrix increased logarithmically with time in the second (slow) stage. It is difficult to make an exact comparison with their

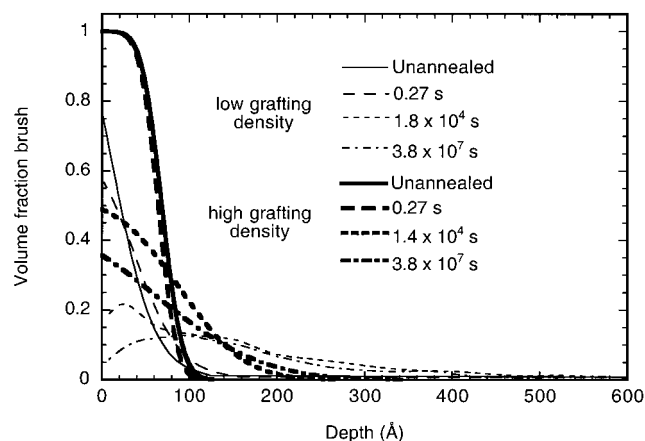


Figure 11. Brush profiles for identical networks ($P=92$) with different grafting densities. The bold lines are for the higher grafting density.

prediction since we can only measure the interfacial width and not the number of segments.

Effect of Cross-Link Density. Figure 10a–e compares brushes with the higher grafting density and different networks after each annealing time. There are some initial differences in the unannealed profiles (due to intrinsic interfacial roughness in the networks). However, after the shortest annealing time (0.27 s), the width of the interface is largest for the lowest cross-linking density and decreases monotonically with increasing density of cross-links. This is as predicted by O & M (eq 5) and Brochard-Wyart⁶ and is in agreement with the experiments of Deruelle et al.,⁴ the tighter the network, the harder it is for the brush to penetrate. Similar behavior is observed after 10 min. In this case two profiles which correspond to times which bracket 10 min are shown for the $P=92$ network, since slightly different annealing times were used. After 1.8×10^4 s, the same trend is observed except that, at this point, the $P=197$ and 461 networks are alike. By the longest annealing time (at which point we believe equilibrium is being approached), all the profiles are very similar; i.e., the equilibrium profile is independent of cross-link density. This contrasts with the work on penetration of high M_w linear polymers into networks,²⁰ where it was shown using a simple mean field theory argument that there should be more penetration of the network for lower cross-linking densities. Similar results are observed for the lower grafting density brush, but since we have only two values of P in this case, we do not discuss them in detail.

Effect of Grafting Density. Figure 11 compares the profiles from sets 2 and 3, which have the same N and P but different grafting densities, for the unannealed, 0.27, 1.4×10^3 , and 1.8×10^3 s, and equilibrium samples. If the profiles for the different grafting densities are compared after the same annealing time, it is apparent that the lower grafting density chains penetrate the network much faster. After the longest anneal when equilibrium is approached, the lower grafting density chains stretch ~ 400 Å into the network, whereas the higher σ ones reach ~ 200 Å. The grafting density clearly has a strong effect; lower σ chains penetrate both more quickly (in agreement with the predictions of Ligoure¹⁴ and O & M^{15,16}) and deeper into the network. Since we have only two values of σ to compare which differ by less than a factor of 2, we cannot say much more. It would be interesting to study a wider range of

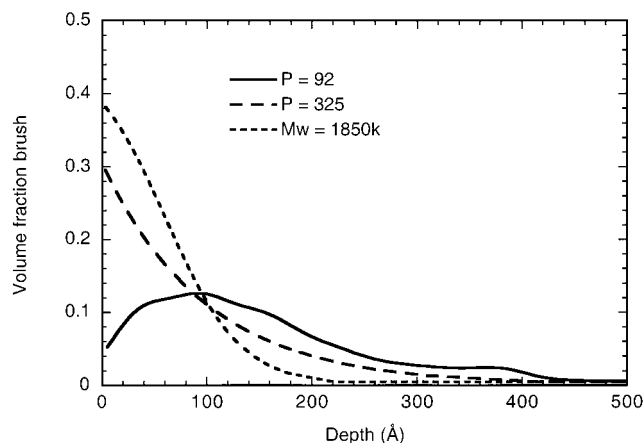


Figure 12. Profiles of a low σ brush in a $P=92$ network, $P=325$ network, and $M_w = 1.85 \times 10^6$ linear polymer after annealing for 3.8×10^7 s (an unscaled time of 165 h at 179.5 °C).

grafting densities to see if the extent of penetration reproduces the maximum that Deruelle et al. found in the fracture toughness.⁴

Comparison with Homopolymer Matrix. The kinetics of penetration of a brush into a homopolymer has been studied previously.¹⁸ It is however interesting to compare the equilibrium profiles of a brush in a permanently cross-linked network and in a high molecular weight linear homopolymer where there are only entanglements. Figure 12 shows the profiles for the low σ brush in a $P=92$ network, a $P=325$ network, and a linear polymer matrix with a molecular weight of 1.85×10^6 after annealing for 3.8×10^7 s (165 h at 179.5 °C). The brush in the homopolymer is less stretched than in the network. This is perhaps surprising since we observed above (Figure 10e) that the equilibrium profile in networks is independent of the cross-link density. In the $P \rightarrow \infty$ limit, i.e., a homopolymer matrix, one might expect to obtain the same brush profile.

To explain this difference we considered and dismissed several effects linked to experimental artifacts:

(i) The brush in the homopolymer is not at equilibrium. We are confident that this is not the case, since the profile is consistent with previous experiments and self-consistent mean-field calculations.²⁴

(ii) The networks could have been prepared in a swollen state, thus causing the brush to penetrate further into them than they would into an unswollen network. However in another experiment,²⁰ it has been shown that high M_w linear homopolymer did not penetrate the $P=45$ networks. In the case of a swollen preparation state, these polymers should have entered the network. We conclude that the preparation state of the network is unlikely to be a significant factor in these experiments.

(iii) It is possible that the brush–network and brush–homopolymer interaction parameters are not the same, due to the different chemical nature of the cross-links. If the PS and the cross-links had a negative interaction parameter, then the brush would be more easily absorbed into the network. However if this were the case, we would expect the equilibrium profile to have a very strong dependence on the cross-link density.

It is therefore very likely that the difference between the equilibrium profiles with homopolymer and network matrixes is real. Without knowing the lateral distribution of network heterogeneities it would be impossible

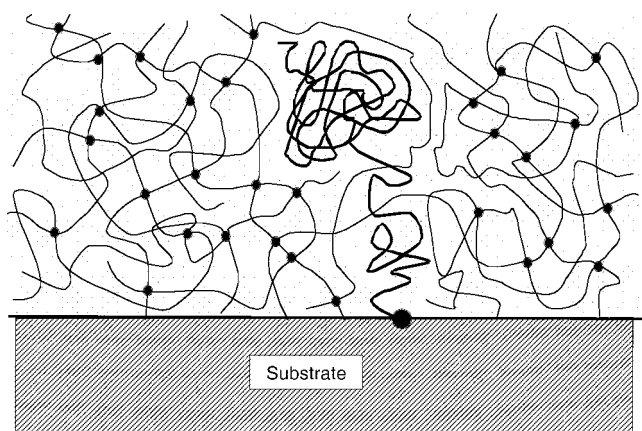


Figure 13. Schematic diagram showing a polymer in the "tadpole" configuration. The thicker lines and larger filled circle represent the tadpole. The thinner lines and smaller circles represent network chains and cross-links.

to isolate the various physical effects that may be causing this difference. Some possible explanations are discussed below:

(a) It has been theoretically predicted³² that a tethered chain could be extended in a random potential (compared with a homogeneous potential). Since the distribution of cross-links is random and that of temporary entanglements is isotropic, this comparison is valid. Grafted chains extending into the network may find a region of low cross-linking density in which they may lower their free energy. Such regions are called entropic traps because the relative lack of cross-links allows an un-cross-linked polymer chain more conformations than in heavily cross-linked regions. As a result, such "soft" regions represent wells where the brush can minimize its free energy. The resulting extension is a compromise between this gain in free energy and the loss in free energy due to the stretching of the brush to reach the well. The long extended chain and the collapsed head of the brush in the well form a similar shape to a tadpole and these structures are thus named. This conformation is schematized in Figure 13.

(b) A brush that does not extend deep into the network will swell that part of the network in which it resides. If the brush extends further into the bulk, the network is less swollen at any one point. It therefore follows that it would be energetically more favorable for the brush to extend deeper into the network. Another way of considering this is that in the melt case the matrix chains can be expelled from the brush interface but a network cannot. To minimize the elastic deformation of the network, the brush chains tend to be extended.

(c) One could interpret the greater penetration of networks rather than linear polymers as evidence of entropy in the networks. The entropy of a polymer network has for some time been a source of great controversy.³³ In the original unswollen network, the cross-links may be taken to be distributed in much the same way as entanglements. When networks are swollen by solvent or by another polymer, heterogeneities become apparent because the regions where cross-linking is lighter will be able to absorb more solvent or polymer than more densely cross-linked regions. This gives rise to an entropy term in the free energy describing this dispersion in the network junctions relative to the original unswollen state. This term encourages

mixing and may therefore explain why the brushes penetrate deeper into the network than a homopolymer matrix.

In all of these cases, one would also expect a cross-linking density dependence on the amount of stretching. However, one can think of effects minimizing this. In the first case of the tadpoles (a), it might be argued that the more heavily cross-linked networks would have more wells for the brush to collapse into than the lightly cross-linked networks. The more cross-linked the network, the more extended the brush. However, in less cross-linked networks, it could well be the case that there could be more brushes in each well (because they may cover a greater volume). There could therefore be two countering effects. In reality it is probably the case that all three effects (a, b, and c) contribute. Without knowledge of the three-dimensional structure of the brushes in the network and the distribution of heterogeneities, it would be difficult to determine the dominant factors.

Conclusions

To summarize, the main findings of our experiments are as follows.

1. We find that the kinetics of penetration of grafted chains into a polymer network follow a two-stage process: there is an initial rapid partial interdigitation, followed by a slow relaxation to equilibrium over several days at elevated temperatures. This is in agreement with the model of O & M,^{15,16} the simulations of Deutsch and Yoon,¹⁷ and the experiments of Reichert and Brown.³ In contrast, Deruelle et al.^{4,5} suggested that equilibrium is reached fairly quickly, although they also admit the possibility of slower kinetics, since their experiments were not very sensitive in this respect. Their active connector model is consistent with the metastable state with partial interdigitation rather than true equilibrium. Partial interdigitation may well strengthen the interface sufficiently for practical purposes. It has been observed that most of the fracture toughness arises in the early stage of annealing,^{3,34} implying that partial interdigitation gives most of the adhesive strength.

2. Increasing the cross-link density of the network slows the kinetics of penetration, in agreement with the predictions of O & M^{15,16} and Brochard-Wyart,⁶ and the experiments of Deruelle et al.^{4,5} We find that the equilibrium profile is independent of cross-link density (over the range that we studied), which is surprising since it might be expected that less penetration would be achieved in the case of more cross-linked networks.

3. Lower grafting density brushes penetrate more quickly than higher σ ones, but necessarily have a different equilibrium profile. Theoretically, it is expected³⁵ that the adhesion is directly proportional to the grafting density. The data of Deruelle et al.⁴ show that the relation is actually more complicated, since there is an adhesion maximum, with the adhesion energy dropping for greater grafting densities. It would be interesting to examine a wider range of grafting densities to study the density profiles of brushes around the adhesion maximum.

4. The equilibrium profile of a brush in a network is different from that in a homopolymer matrix. We speculate that this may be because the entropy of mixing for a brush penetrating a network is greater than that for a homopolymer matrix. It is also suggested

that because networks cannot be expelled by a brush in the way that linear polymers can, the brush is extended in order to minimize the swelling. A final possibility is due to heterogeneities in the network; the brush extends itself to find less cross-linked regions where it has more conformations.

These results help us to understand the phenomena at the interface, by providing a microscopic picture of the behavior of the tethered chains, which allows us to test existing models. Future work should aim to measure the interfacial profile and interfacial adhesion using the same sample for both experiments.³⁴ It would be very interesting to perform such experiments for a brush and a network.

Acknowledgment. C.J.C. wishes to thank Trinity College, Cambridge, U.K., for support, in the form of a research fellowship. M.G. would like to thank the European Union for support under the Human Capital and Mobility scheme while at the L.L.B. In Freiburg, M.G. was supported with a fellowship from the Alexander von Humboldt Stiftung. We thank J. Suhm and F. Dietsche of the Freiburger Materialforschungszentrum for their help and advice in preparing some of the networks. We should also like to thank Dr. J.-U. Sommer and Professors T. C. B. McLeish and M. E. Cates for helpful discussions.

References and Notes

- (1) Brown, H. R. *IBM J. Res. Dev.* **1994**, *38*, 379.
- (2) Léger, L.; Hervet, H.; Raphaël, E. *Adv. Polym. Sci.* **1999**, *138*, 199.
- (3) Reichert, W. F.; Brown, H. R. *Polymer* **1993**, *34*, 2289.
- (4) Deruelle, M.; Léger, L.; Tirrell, M. *Macromolecules* **1995**, *28*, 7419.
- (5) Deruelle, M.; Tirrell, M.; Marciano, Y.; Hervet, H.; Léger, L. *Faraday Discuss.* **1994**, *98*, 55.
- (6) Brochard-Wyart, F.; de Gennes, P. G.; Léger, L.; Marciano, Y.; Raphaël, E. *J. Phys. Chem.* **1994**, *98*, 9405.
- (7) Brown, H. R. *Faraday Discuss.* **1994**, *98*, 47.
- (8) Mhetar, V.; Archer, A. *Macromolecules* **1998**, *31*, 8607.
- (9) Mhetar, V.; Archer, A. *Macromolecules* **1998**, *31*, 8617.
- (10) Durliat, E.; Hervet, H.; Léger, L. *Europhys. Lett.* **1997**, *38*, 383.
- (11) Massey, G.; Hervet, H.; Léger, L. *Europhys. Lett.* **1998**, *43*, 83.
- (12) Rubinstein, M.; Adjari, A.; Leibler, L.; Brochard-Wyart, F.; de Gennes, P. G.; Pincus, P. *C. R. Acad. Sci. Paris* **1993**, *316*, 317.
- (13) Ji, H.; de Gennes, P.-G. *Macromolecules* **1993**, *26*, 520.
- (14) Ligoure, C. *Macromolecules* **1996**, *29*, 5459.
- (15) O'Connor, K. P.; McLeish, T. C. B. *Macromolecules* **1993**, *26*, 7322.
- (16) O'Connor, K. P.; McLeish, T. C. B. *Faraday Discuss.* **1994**, *98*, 67.
- (17) Deutsch, J. M.; Yoon, H. *Macromolecules* **1994**, *27*, 5720.
- (18) Clarke, C. J. *Polymer* **1996**, *37*, 4747.
- (19) Doi, M.; Edwards, S. F. *The Theory of Polymer Dynamics*; Clarendon Press: Oxford, U.K., 1986.
- (20) Geoghegan, M.; Boué, F.; Bacri, G.; Menelle, A.; Bucknall, D. G. *Eur. Phys. J. B* **1998**, *3*, 83.
- (21) The value of τ_1 was estimated from measurements of the bulk tracer diffusion coefficient of polystyrene (Mills, P. J.; Green, P. F.; Palmström, C. J.; Mayer, J. W.; Kramer, E. J. *Appl. Phys. Lett.* **1984**, *45*, 957.) scaled to 150 °C.
- (22) de Gennes, P. G. *J. Phys.* **1975**, *36*, 1199.
- (23) Klein, J. *Macromolecules* **1986**, *19*, 105.
- (24) Clarke, C. J.; Jones, R. A. L.; Edwards, J. L.; Shull, K. R.; Penfold, J. *Macromolecules* **1995**, *28*, 2042.
- (25) Zielinski, F.; Buzier, M.; Lartigue, C.; Bastide, J.; Boué, F. *Prog. Colloid Polym. Sci.* **1992**, *90*, 115.
- (26) Ramzi, A.; Zielinski, F.; Bastide, J.; Boué, F. *Macromolecules* **1995**, *28*, 3570.
- (27) Russell, T. P. *Mater. Sci. Rep.* **1990**, *5*, 171.
- (28) Jones, R. A. L.; Norton, L. J.; Shull, K. R.; Kramer, E. J.; Felcher, G. P.; Karim, A.; Fetters, L. J. *Macromolecules* **1992**, *25*, 2359.
- (29) Sivia, D. S.; Hamilton, W. A.; Smith, G. S. *Physica B* **1991**, *173*, 121.
- (30) Geoghegan, M.; Jones, R. A. L.; Sivia, D. S.; Penfold, J.; Clough, A. S. *Phys. Rev. E* **1996**, *53*, 825.
- (31) Ferry, J. D. *Viscoelastic Properties of Polymers*, 3rd ed.; Wiley: New York, 1980.
- (32) Cates, M. E.; Ball, R. C. *J. Phys.* **1988**, *49*, 2009.
- (33) Flory, P. J. *Proc. R. Soc. London, A* **1976**, *351*, 351.
- (34) Schnell, R.; Stamm, M.; Creton, C. *Macromolecules* **1998**, *31*, 2284.
- (35) Raphaël, E.; de Gennes, P. G. *J. Phys. Chem.* **1992**, *96*, 4002.

MA982020F